  Bull. Chem. Soc. Jpn., 65, 739—745 (1992)

The Crystal Structures of Cyanide Metmyoglobins Reconstituted with Iron(III) Complexes of Porphyrin, 5,10,15,20-Tetramethylporphyrin, and 5,10,15,20-Tetraethylporphyrin

Takao SATO,* Nobuo TANAKA, Hideaki MORIYAMA, Osamu MATSUMOTO, Akio TAKENAKA, Saburo NEYA,† and Noriaki FUNASAKI†

Department of Life Sciences, Faculty of Bioscience and Biotechnology, Tokyo Institute of Technology, 4259 Nagatsuta, Midori-ku, Yokohama 227

† Department of Physical Chemistry, Kyoto Pharmaceutical University, Yamashina-ku, Kyoto 607

(Received October 18, 1991)

The structures of three mimic myoglobins reconstituted with synthesized iron(III) meso-substitututed porphyrins have been studied by X-ray crystallography. Although the overall structure of each globin was the same as that of the native, apart from a few terminal residues, the C_α atom of Arg45 in each crystal was displaced by 2.7 Å from that in the native. This large displacement opens a channel for the ligand penetration, formed by His64, Thr67, Val68, and heme. The movement of each porphyrin was estimated from the refined anisotropic temperature factors of its atoms, which showed that the root-mean-squares amplitude of the vibration about the normal to the porphyrin plane was significantly larger than the globin's movement.

Myoglobin is composed of a single peptide chain and a non-covalently bound protoheme,[1] and contributes to the internal respiratory and preservation of molecular oxygen in heart and skeletal muscles. The detailed molecular geometries of the hemes and their protein environments in myoglobins have been studied by X-ray crystal structure analysis in order to explain the mechanism of ligand formation and its effect on protein conformation.[2-6] The results indicated that the heme was kept inside a globin by the interaction of its peripheral substituents with the protein, which implies that these interactions are essential for the function of myoglobin. In these structures, however, no obvious pathway was found through which a ligand molecule can come to the heme's distal side from the exterior. It was proposed that rapid fluctuations in the protein structure open the transient channel for ligand penetration,[7] and the importance of the residues around the heme was emphasized by Ringe et al.[8] as a molecular doorstop mechanism.

Several kinds of less bulky hemes were synthesized by introducing identical alkyl groups at 5,10,15,20-positions of porphyrins[9] (Fig. 1). These hemes have no propionic acid substituents and cannot form a hydrogen bond with Arg45 in the protein heme pocket. The bulkiness of substituents was varied as propyl, ethyl, methyl moieties, and hydrogen atom in order to study the effect of the interaction between the heme and globin. From the temperature dependent NMR studies,[9-10] the less bulky porphyrin ring was observed to rotate about the Fe–N^ε (His93) bond at lower temperatures, and at 20 °C in case of the porphyrin myoglobin, where the X-ray data were collected. These results indicated that the structures of a series of mimic molecules with different sizes of porphyrins may clarify the interaction between the heme and globin. The present paper reports the three dimensional structures of cyanide metmyoglobin reconstituted with iron(III) complexes of porphyrin and 5,10,15,20-tetramethylporphyrin and 5,10,15,20-tetraethylporphyrin determined by X-ray crystallography. Structural comparisons between the native and reconstituted proteins will throw light on the function of myoglobin.

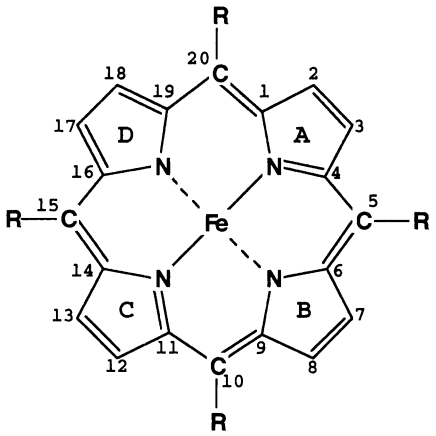

R = H	Porphyrin
R = CH_3	Tetramethylporphyrin
R = C_2H_5	Tetraethylporphyrin
R = C_3H_7	Tetrapropylporphyrin

Fig. 1. Chemical structures of iron(III) complexes of porphyrin and 5,10,15,20-tetraalkylporphyrins. The R is H for porphyrin, methyl for tetramethylporphyrin, and ethyl for tetraethylporphyrin. The pyrrole ring designated as A is exposed from the globin.

Materials and Methods

Preparation of the Materials: The porphyrins, 5,10,15,20-tetramethylporphyrin, and 5,10,15,20-tetraethylporphyrin were synthesized from pyrrole and R–CHO(R = H, Me, or Et), and purified on a silica-gel column.[11-12] The iron complex was produced by refluxing porphyrin and iron(III) chloride in

N,*N*-dimethylformamide.[13] After iron oxidation with air, the synthetic heme was purified through a silica-gel column ($CHCl_3$: CH_3OH 90 : 10 (v/v)). Apomyoglobin was prepared by the methyl ethyl ketone method from sperm whale myoglobin purchased from Sigma (TypeII).[14] The mimic myoglobins reconstructed with iron(III) complexes of synthesized porphyrins were purified on carboxymethylated cellulose columns (Whatman, CM-52). A small amount of sodium cyanide was added to the purified metmyoglobin to stabilize the reconstituted molecule. The myoglobins utilized in the present study had a $A_{419\,nm}/A_{280\,nm}$ ratio of 3 or greater.

Crystallization: The three mimic myoglobins reconstructed with iron(III) complexes of porphyrin, 5,10,15,20-tetramethylporphyrin, and 5,10,15,20-tetraethylporphyrins (PorMb, TMePMb, and TEtPMb, hereafter) were crystallized by either a microdialysis method or a hanging drop vapor diffusion method. Protein solution which was composed of 10% (w/v) protein, 32—43% (w/v) ammonium sulfate and 10 mM sodium cyanide (1M=1 mol dm^{-3}) in 0.1 M Tris-HCl solution at pH 7.0 was equilibrated against the same buffer solution of 75% ammonium sulfate. Crystals suitable for X-ray analysis grew after several weeks at 5 °C.

Data Collection: Preliminary crystallographic data for each myoglobin were determined from precession photographs (Table 1). In the cases of PorMb and TEtPMb, diffraction data were collected at 20 °C on a Rigaku four circle diffractometer with nickel-filtered Cu-$K\alpha$ radiation generated by a rotating anode generator operating at 40 kV–200 mA. The ω-scan mode was applied with a scanning speed of 4 ° min^{-1} and a scan width of $(0.7+0.4\tan\theta)°$. Background intensities were counted for 3 or 4 s at each end of the scan. Three standard reflections were measured every 100 reflections during data collection to monitor the crystal decay and slippage. About five thousand intensity data were collected from each crystal, before observed structure amplitude of any standard reflection was reduced by more than 10%. After the correction for decay effect as a function of the elapsed time and absorption effect by the North–Phillips method,[15] a set of data for each protein was completed by scaling the data of different crystals by the Sparks–Rollet method.[16]

The data of TMePMb were collected with the synchrotron radiation at the Photon Factory in National Labratory for High Energy Physics, utilizing the Weissenberg camera developed by Prof. N. Sakabe et al., which uses an imaging plate as the X-ray detector.[17] A crystal with dimensions of $0.2\times0.05\times0.1$ mm^3 was set with *b* axis along the spindle axis of the goniometer. The reflections were recorded at 20 °C. For each plate the spindle axis was scanned by 7.8° with an exposure time of 15 s, and consecutive scans were overlapped by 0.4°. After the digitallization of each plate with Fuji Film BA-100 IP scanners, the intensity of each reflection was evaluated by the program 'WEIS'.[18] All observed data were gathered into a file by the program 'COMBINE',[18] and were scaled by the program 'SCALE'.[18] A total of 7035 unique reflections were observed out of 17444 measured reflections within 1.8 Å resolution. All of these calculations were carried out on a FACOM VP-400 computer at the Photon Factory.

Table 1. Crystal Data of Mimic Myoglobins Reconsituted with Iron(III) Porphyrins

Compound	Space group	Cell parameters		
		a	*b*	*c*
		Å	Å	Å
PorMb	$P2_12_12_1$	57.85	76.10	33.84
TMePMb	$P2_12_12_1$	58.85	76.58	34.05
TEtPMb	$P2_12_12_1$	58.07	76.69	33.48

Structure Analysis and Refinement

Each structure was solved by the molecular replacement method. The starting model, composed of only a globin's structure of mimic myoglobin reconstructed with iron(III) 5,10,15,20-tetrapropylporphyrin (TPrPMb, hereafter),[19] was located and oriented as a rigid body so as to minimize the *R* factor between the observed and calculated structure factors from 5 to 2.2 Å resolution with the simplex method.[20] The results confirmed that each molecule was isomorphous with TPrPMb. The structures of the globins were refined by the program PROFFT,[21] which is an implementation of Hendrickson's restrained least squares method.[22] After several cycles of refinement without porphyrins, difference Fourier maps were calculated to locate the iron(III) porphyrin complex. In each map, the prominent peak could be assigned for an iron atom. For TEtPMb, and TMePMb, the in-plane orientations of the porphyrin rings were determined by assigning the protruding peaks to the alkyl groups. For PorMb, however, the doughnut-like flattened density map around the iron atom made it difficult to fix the orientation of the heme without ambiguity. The cyano group coordinating to the iron atom did not appear on any Fourier maps, although the absorption spectra indicated the presence of CN^- ions in solution. The refinements, including porphyrins, were continued with individual temperature factors but without water molecules. The *R* factors converged to 24, 25, and 22% for TEtPMb, TMePMb, and PorMb, respectively. The weighting parameters for various observational classes are listed in Table 2 along with the results of refinement. The anisotropic temperature factors of the iron and porphyrin's skeletal atoms were succesively refined, fixing the positional parameters of the porphyrin ring's atoms and all parameters of the globin's atoms. The mobility of the heme was estimated by Cruickshank's rigid body analysis.[23] The root-mean-squares amplitudes of rotation and vibration of porphyrins calculated from the anisotropic temperature factors are listed in Table 3.

Results and Discussion

The protein was purified by completely removing the uncomplexed porphyrin and globin to obtain crystals suitable for X-ray analysis. Reconstituted myoglobins utilized in the present study were of high purity with $A_{419\,nm}/A_{280\,nm}$ ratios greater than 3.

Each modified heme was found to be inserted into the globin in a similar way as the native. The symmetrical character of the porphyrins allows no ambiguity as to the inserted orientation of the porphyrins. The positions of the iron atom in respect to the globin were shifted from the native by 0.4 Å for PorMb, 0.3 Å for TMePMb, and 0.8 Å for TEtPMb towards the exterior. With the shift of 0.8 Å for TPrPMb, the results indicate that the bulky substituents push the porphyrins outward, in proportion

Table 2. Statistics of Least-Square Refinement

Number of cycles	43		19		21	
Resolution/Å	5.0—2.2		5.0—2.2		5.0—2.2	
Number of reflections	5007		7035		5389	
Threshold for inclusion	$I \geqslant 3\sigma$ (I)		$I \geqslant 3\sigma$ (I)		$I \geqslant 3\sigma$ (I)	
Final R factor[a)]	0.217		0.255		0.238	
	Target σ	rms Δ	Target σ	rms Δ	Target σ	rms Δ
Distances/Å						
Bonds	0.030	0.044	0.020	0.020	0.020	0.017
Angles	0.040	0.069	0.030	0.043	0.030	0.036
Dihedral	0.050	0.067	0.050	0.054	0.050	0.053
Planes/Å	0.030	0.035	0.020	0.016	0.020	0.012
Chiral centers/Å^3	0.100	0.300	0.150	0.204	0.150	0.188
Contacts/Å						
Single	0.300	0.264	0.500	0.217	0.500	0.228
Multiple	0.300	0.252	0.500	0.274	0.500	0.273
H-bonded (X···Y)	0.300	0.291	0.500	0.297	0.500	0.262
Torsion angle/°						
Omega	5.0	5.3	3.0	2.6	3.0	2.2
Chi	15.0	25.4	15.0	23.8	15.0	24.7
Aromatic	15.0	37.2	20.0	39.9	20.0	37.5
Thermal parameters B/Å^2						
Main bonded	1.0	0.787	0.050	0.032	0.050	0.033
Main angle	1.5	1.296	0.100	0.060	0.100	0.063
Side bonded	1.0	0.830	0.050	0.050	0.050	0.040
Side angle	1.5	1.362	0.100	0.023	0.100	0.023
Restrains against excessive shift						
Positional parameters/Å	0.1		0.1		0.1	
Thermal parameters/Å^2	3.0		3.0		3.0	
Reduction of van der Waals contact distances/Å						
Single	0.3		0.3		0.3	
Multiple	0.0		0.0		0.0	
H-bond	0.2		0.2		0.2	

a) $R=\Sigma_{h,k,l}||F_o|-|F_c||/\Sigma_{h,k,l}|F_o|$.

Table 3. Root-Mean-Squares Amplitudes of Translational and Rotational Motion along the Three Orthogonal Axes[a)]

	Tx	*Ty*	*Tz*	*T'*	*Rx*	*Rx*	*Ry*	*Ry*	*Rz*	*Rz*	*R'*
	Å	Å	Å	Å	°	Å	°	Å	°	Å	°
PorMb	0.5	0.4	0.9	0.3	4.0	(0.3)	2.5	(0.2)	0.4	(0.0)	1.2
TMePMb	0.5	0.5	0.8	0.4	2.3	(0.1)	1.4	(0.1)	0.4	(0.0)	0.4
TEtPMb	0.5	0.5	0.5	0.4	2.3	(0.1)	3.0	(0.2)	0.4	(0.0)	0.4
TPrPMb	0.7	0.6	0.4	0.2	4.9	(0.3)	0.4	(0.0)	0.4	(0.0)	1.3

a) T and R represent the amplitudes of translation and rotation in respect with the corresponding axes. The figures in brackets correspond to the movement of residues away from the iron atom by 3.5 Å.

to its bulkiness. The inserted porphyrins were tilted from the native protoheme by 8°(PorMb), 5.6°(TMePMb), and 8.6°(TEtPMb). As discussed in TPrPMb,[19] the electron density distributions on the porphyrin planes were not clear, probably due to the mobility of the porphyrin, though the globins were determined definitely. The invisibility of the cyano group was attributed to this indistinct distribution. For TMePMb and TEtPMb, the porphyrins were located on the electron density distributions by assigning the peripheral peaks for the substituents, and were found to rotate around its normal from the native by 30°, as found in TPrPMb. In case of PorMb which has hydrogen atoms at four meso positions, the observed electron density distribution was weak and doughnut-like, which suggests the porphyrin moves around its averaged position. The average isotropic temperature factors for the porphyrin ring atoms were calculated to be 19.8 Å^2 (PorMb), 15.7 Å^2 (TMePMb), and 16.7 Å^2 (TEtPMb), those of the C_α atoms being 8.0, 7.7, and 8.0 Å^2,

Table 4. Root-Mean-Squares Displacement of Residues at Heme Environment[a)]

Compound	Overall	Arg45	Phe46	Leu89	Lys96	Ile99
	Å	Å	Å	Å	Å	Å
PorMb	0.6	2.9	0.8	1.0	1.8	0.9
TMePMb	0.6	3.1	0.7	1.0	2.0	0.9
TEtPMb	0.6	3.1	0.8	0.9	1.8	0.8

a) The figures are distances calculated after fitting the mimic molecules on the native.

Table 5. Geometry of Porphyrin, His64 and His93

From	To	PorMb	TMePMb	TEtPMb	TPrPMb	Native
		Å	Å	Å	Å	Å
Fe	Porphyrin plane	0.13	0.01	0.18	0.07	0.27
Fe	His64 $N^{\varepsilon 2}$	5.05	5.00	4.61	5.10	4.67
Fe	His93 $N^{\varepsilon 2}$	2.40	2.84	2.41	2.22	2.13
His64 $N^{\varepsilon 2}$	Porphyrin plane	4.38	4.34	4.23	4.42	4.22
His93 $N^{\varepsilon 2}$	Porphyrin plane	2.46	2.73	2.30	2.22	2.39

a) Calculated from the coordinates of the BNL data base.[4)]

respectively. These results also indicate that the porphyrin is more mobile than globin in the modified molecules, and the porphyrin of PorMb moves more than the others. These observations were also supported by the calculation of the rotational potential energy about His93C^{ε}–His93N^{ε}–Fe–HemeCCD with MM2, as reported previously.[19)]

The structures of the globins in the modified myoglobins were similar to that in the native protein, although they do not have the same crystal symmetry. Table 4 shows the root-mean-squares derivations among them after superposing the C_{α} atoms with one another by the least squares method. The overall displacements in the Table indicate that different sizes of substituents on porphyrins do not perturb the structures of the globins so much. Although each molecule kept the same geometry of the groups indispensable to the function (Table 5), the detailed structures varied from the native in several parts of the chain foldings. The large deviation of the seven or eight C-terminal residues reflects the fact that they are buried between the molecules in the native, and are exposed to the solvent in the modified proteins owing to the different crystal packing. Several residues neighboring the porphyrin were displaced from the native significantly, in company with the varied tiltings of the porphyrins, as shown in Table 5. In each modified myoglobin, the C_{α} atom of Arg45 on the CD loop was displaced from that that of the native by 2.9—3.1 Å, because its guanidino group has no hydrogen bond via water molecule with the carboxyl group of the propionic acid which was deleted from the synthetic porphyrin. Phe46 on the same loop moved in company with Arg45. They were exposed to the solvent region and opened a channel through which ligand molecule may gain access to the heme plane. On the FG loop, the remarkable shift of Lys96 (2.0 Å) in the

Table 6. The Interatomic Distances between Carbons or Alkyl Groups at the Meso-Positions of Porphyrin and Surrounding Residues[a)]

From	To	PorMb	TMePMb	TEtPMb
		Å	Å	Å
5-Carbon	His 64 $C_{\varepsilon 1}$	3.75	3.75	3.89
	His 97 $N_{\varepsilon 2}$	3.90	4.06	4.36
10-Carbon	Leu 89 $C_{\delta 2}$	3.68	3.60	4.26
	His 93 $N_{\varepsilon 2}$	3.75	3.78	3.19
15-Carbon	His 93 $C_{\delta 2}$	4.11	4.60	3.58
	Leu 104 $C_{\delta 2}$	3.37	4.02	4.53
20-Carbon	Phe 43 C_{ζ}	3.70	3.72	4.64
	His 97 C_{β}	4.36	4.43	3.58
	His 97 C_{γ}	4.55	4.47	3.40
	Ile 99 $C_{\gamma 1}$	3.61	3.81	4.76
5-Methyl[b)]	His 64 $C_{\varepsilon 1}$		4.23	3.81
	His 97 $N_{\varepsilon 2}$		3.91	4.88
10-Methyl[b)]	Val 68 $C_{\gamma 1}$		3.51	4.27
	Leu 89 $C_{\delta 2}$		4.28	3.87
15-Methyl[b)]	Ile 99 $C_{\gamma 2}$		4.83	3.87
	Tyr 103 O		3.71	4.49
	Leu 104 $C_{\delta 2}$		2.92	4.41
10-Methyl[b)]	Lys 42 O		3.86	3.12
	Phe 43 C_{ζ}		3.32	5.24
	Phe 43 $C_{\delta 1}$		4.00	4.51
	His 97 C_{β}		4.93	3.38
	Ile 99 $C_{\delta 1}$		3.84	4.77
5-Ethyl[c)]	His 64 $C_{\varepsilon 1}$			3.00
10-Ethyl[c)]	Val 68 $C_{\gamma 1}$			3.51
20-Ethyl[c)]	Lys 42 O			2.46
	Phe 43 C_{α}			3.76

a) The table includes the distances in unit of Å, which are less than 4.0 Å in either of three molecules. b) Methylene carbon of ethyl group. c) Methyl carbon of ethyl group.

proximal pocket is responsible for intermolecular interactions with an adjacent molecule in the crystal. Another large deviation from the native was found at Leu89 (1.0 Å) which loosens the porphyrin in the globin, and at Ile99 (0.9 Å) which alters the location of the C-terminal helix by removing the hydrogen bond with Tyr166 in the helix.

There are several contacts between the alkyl groups of the porphyrins and the surrounding residues of globins as shown in Fig. 2. Their distances in the three molecules are listed in Table 6. In TEtPMb, ethyl groups lie above the porphyrin plane with staggered conformations, and make contact with the distal histidine (His64) at the 5-position, Val68 at the 10-position, and Lys42 and Phe43 at the 20-position. In TMePMb and PorMb, the situations around the porphyrin were not varied in spite of the smaller protruding groups at the meso positions. These facts imply that the porphyrins do not fit tightly to the globin as reported in TPrPMb.

The two step mechanism for the reaction of myoglobin with small ligand molecules such as O_2 or CO[24] points out that the ligand gains access to the iron atom from the heme distal side through the globin, and subsequently binds with the iron atom. To inquire into the relation between this mechanism and the three dimensional structure, the volume of the pathway at the distal side, named the vacancy space, was calculated by integrating unoccupied space within the sphere of radius of 10 Å from the heme iron. In the calculation, the Fe atom was treated as a sphere of covalent radius (0.79 Å), and the other atoms were treated as spheres of van der Waals radii of 1.55 Å for C, 1.40 Å for O, and 1.50 Å for N.[25] The estimated volumes of the spaces for mimic molecules, 398.8 Å^3 for PorMb, 426.1 Å^3 for TMePMb, 438.3 Å^3 for TEtPMb, and 450.3 Å^3 for TPrPMb were larger than 385.9 Å^3 of the native. It is plausible that the accessibility of the ligand molecule to the iron atom is concerned with the binding reaction, because the mimic myoglobins react faster with CO, the vacancy spaces are larger as described elsewhere.[26]

The atoms of the porphyrins in each mimic molecule were refined with anisotropic temperature factors in order to estimate the movement of porphyrins using the Cruickshank's rigid body least squares method,[23] each ring undergoing translational and rotational motion as a whole. The calculation is accurate enough to allow

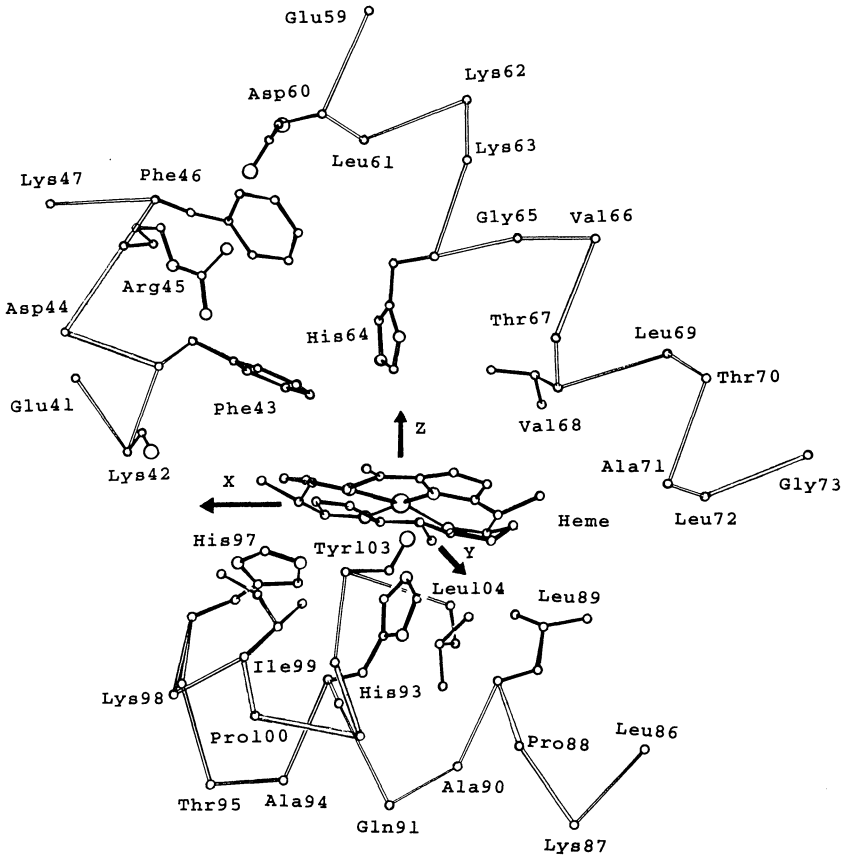

Fig. 2. Heme environmental stucture of iron(III) 5,10,15,20-tetramethylporphyrin myoglobin. The figure shows the C_α-tracing and the amino acid residues around porphyrin. The pathway through which CO ligand was presumed to enter the pocket, lies among Arg-45, His-64, Val-68, and the heme group. The axes x, y, and z are in Fig. 3.

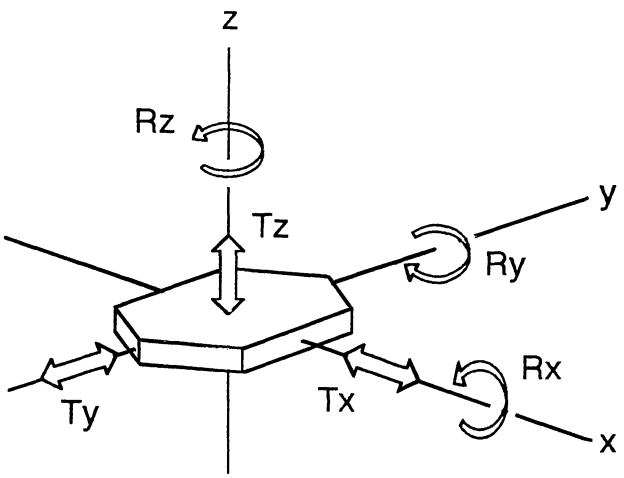

Fig. 3. Schematic diagrams defining the orthogonal axes on the porphyrin plane for rotational and translational analysis. Straight arrows indicate translational axes and lines with "circular" arrows around them represent librational axes, as discussed in the text.

qualitative discuss of the motions of the porphyrin. Quantitative discussion, however, is difficult because all the positional parameters and isotropic temperature factors of the globin's atom were fixed to save the computation time during the refinements. The motion can be expressed using two symmetric tensors T and ω, where T represents the anisotropic amplitude of the translation of the rigid body and ω is its anisotropic amplitude of angular motion around the axes through the origin. In the present analysis, the origin was fixed at the iron atom. The z-axis was normal to the porphyrin's least squares plane, the x-axis was passed through the 5,15-carbons and the y-axis was normal to the x and z axes with a right handed system (Fig. 3). In order to assess these movements, the averaged mobility of globin as a whole was estimated from the isotropic temperature factors of the C_α atoms, because they had the smallest temperature factors in each residue. The temperature factor of each C_α atom was thought to be additive of isotropic translation and rotation.

$$<U^2>=t^2+(\omega\times|r|)^2$$

where r is a positional vector of each atom, and t and ω are the translational and rotational amplitudes, respectively. The rotation of the porphyrin around its normal was 0.4° for each case, which was the same as the globins, though the NMR study in solution suggested that the porphyrin rotates around its normal in the pocket. In the crystal, the rotation around the normal to the plane (Rz) may be suppressed by Leu149 of the neighboring molecule ($1/2-x$, $1-y$, $1/2+z$), which contacts with the carbon atoms at the 2- and 3-positions of the pyrrole ring A. The shortest distances between Leu149 and the pyrrole ring A were 5.3 Å for PorMb, 5.2 Å for TMePMb, and 4.4 Å for TEtPMb. The rotation around inplane axes was significantly bigger than those of the globins. It is noteworthy that the rotation around the y axis (Ry) varies the space available for holding the ligand molecule beside the distal histidine, and is concerned with the binding reaction. For PorMb and TMeMb, the amplitudes of the translation along the normal to the porphyrin planes (Tz) were two times as large as that of the globin, and were inversely proportional to the bulkiness of the heme substituents as shown in Table 3. In cases of TMePMb and TEtPMb, the amplitudes of Tz correspond to the subtracted distance between the porphyrin ring and Val68 by their van der Waals distances. In case of PorMb, however, the amplitude (0.92 Å) is beyond the subtracted distances(0.43 Å), which means that this motion transiently compresses the CO binding domain and will affect the ligand binding.

In the present paper, the function of myoglobin has been discussed from the structures and mobilities of mimic metmyoglobins reconstructed with synthetic porphyrins. Although it is obvious that the structure of deoxy form is essential to understand its function, these discussions are valid, since the crystal structures of both forms in the native myoglobin are similar to each other. However, the research will be expanded to the structure determination of deoxy forms of mimic myoglobin for exact discussion.

The calculations were undertaken with the ACOS-930 computer of the Institute for Protein Research, Osaka University and the Micro Vax II of the Faculty of Bioscience and Biotechnology, Tokyo Institute of Technology.

The authors wish to express their thanks to Professors Yukiteru Katsube, Yoshiki Matsuura, Masami Kusunoki, and Yasuyuki Kitagawa of the Institute for Protein Research, Osaka University for their valuable suggestions and permission to use their computers. Thanks are due to Professor Noriyoshi Sakabe, Drs. Atsushi Nakagawa, Nobuhisa Watanabe, and Sou Iwata of the Photon Factory, National Laboratory for High Energy Physics for their guidances and technical assistances of the data collection with the Weissenberg camera. The authors are also grateful to Dr. Keiichi Namba of the Houtani project ERATO for permission to use the BA100 in his laboratory, and Dr. Tadashi Hata of the Analytical and Metabolite Research Laboratories, Sankyo Co., Ltd., for his encouragement and discussions through this study.

This work was partly supported by Grand-in-Aids for Scientific Research Nos. 61304062 and 01440090 from the Ministry of Education, Culture and Science.

References

1) M. Dautrevaux, Y. Boulonger, K. Han, and G. Biserte, *Eur. J. Biochem.*, **11**, 267 (1969).
2) M. F. Perutz, *Br. Med. Bull.*, **32**, 195 (1976).

3) J. C. Kendrew, R. E. Dickerson, B. E. Strandberg, R. G. Hart, D. R. Davies, D. C. Phillips, and V. C. Shore, *Nature,* **185**, 422 (1960).
4) T. Takano, *J. Mol. Biol.,* **110**, 537 (1977).
5) T. Takano, *J. Mol. Biol.,* **110**, 569 (1977).
6) S. E. V. Phillips, *Nature,* **273**, 247 (1978).
7) D. A. Case and M. Karplus, *J. Mol. Biol.,* **123**, 697 (1978).
8) D. Ringe, G. A. Petsko, D. E. Kerr, and P. R. Ortiz de Montellano, *Biochemistry,* **23**, 2 (1984).
9) S. Neya and N. Funasaki, *J. Biol. Chem.,* **262**, 6725 (1987).
10) S. Neya and N. Funasaki, *Biochim. Biophys. Acta,* **952**, 150 (1988).
11) A. Ulman, J. Galluci, D. Fisher, and J. A. Ibers, *J. Am. Chem. Soc.,* **102**, 6852 (1980).
12) A. Ulman, D. Fisher, and J. A. Ibers, *J. Heterocycl. Chem.,* **19**, 409 (1980).
13) A. D. Adler, F. R. Longo, F. Kampas, and J. Kim, *J. Inorg. Nucl. Chem.,* **102**, 6852 (1970).
14) T. Asakura and T. Yonetani, *J. Biol. Chem.,* **244**, 4573 (1969).
15) A. C. T. North, D. C. Phillips, and F. S. Mathews, *Acta Crystallogr., Sect. A,* **24**, 351 (1968).
16) J. S. Rollett and R. A. Sparks, *Acta Crystallogr.,* **13**, 273 (1960).
17) N. Sakabe, *Nucl. Instrum. Methods,* **A303**, 448 (1991).
18) T. Higashi, *J. Appl. Cryst.,* **22**, 9 (1989).
19) T. Hata, Y. Hata, T. Sato, N. Tanaka, S. Neya, N. Funasaki, and Y. Katsube, *Bull. Chem. Soc. Jpn.,* **64**, 821 (1991).
20) "HITAC Mathematical Subprogram Library," Hitachi, Tokyo (1978), Part 3.
21) B. C. Finzel, *J. Appl. Crystallogr.,* **20**, 53 (1987).
22) W. A. Hendrickson, *Methods Enzymol.,* **115**, 252 (1985).
23) D. W. J. Cruickshank, *Acta Crystallogr.,* **9**, 754 (1959).
24) T. E. Carver, R. J. Rohlfs, J. S. Olson, Q. H. Gibson, R. S. Blackmore, B. A. Springer, and S. G. Sligar, *J. Biol. Chem.,* **265**, 20007 (1990).
25) L. Pauling, "The Nature of the Chemical Bond," 3rd ed, Cornell University Press, Ithaca, N. Y. (1960), p. 260.
26) T. Sato, N. Tanaka, S. Neya, N. Funasaki, T. Iizuka, and Y. Shiro, *Biochim. Biophys. Acta,* in press.